Sensitivity Analysis of the Orthoglide: A 3-DOF Translational Parallel Kinematic Machine

Stéphane Caro, Philippe Wenger, Fouad Bennis, Damien Chablat

SENSITIVITY ANALYSIS OF THE ORTHOGLIDE, A 3-DOF TRANSLATIONAL PARALLEL KINEMATIC MACHINE

Stéphane Caro, Philippe Wenger, Fouad Bennis, Damien Chablat
Institut de Recherche en Communications et Cybernétique de Nantes *
1, rue de la Noë - 44321 Nantes, France
Stephane.Caro@irccyn.ec-nantes.fr

ABSTRACT

In this paper, two complementary methods are introduced to analyze the sensitivity of a three degree-of-freedom (DOF) translational Parallel Kinematic Machine (PKM) with orthogonal linear joints: the Orthoglide. Although these methods are applied to a particular PKM, they can be readily applied to 3-DOF Delta-Linear PKM such as ones with their linear joints parallel instead of orthogonal. On the one hand, a linkage kinematic analysis method is proposed to have a rough idea of the influence of the length variations of the manipulator on the location of its end-effector. On the other hand, a differential vector method is used to study the influence of the length and angular variations in the parts of the manipulator on the position and orientation of its end-effector. Besides, this method takes into account the variations in the parallelograms. It turns out that variations in the design parameters of the same type from one leg to another have the same effect on the position of the end-effector. Moreover, the sensitivity of its pose to geometric variations is a minimum in the kinematic isotropic configuration of the manipulator. On the contrary, this sensitivity approaches its maximum close to the kinematic singular configurations of the manipulator.

Keywords: Parallel Kinematic Machine, Sensitivity Analysis, Kinematic Analysis, Kinematic Singularity, Isotropy.

NOMENCLATURE

$\mathcal{R}_b(O,x,y,z)$: reference coordinate frame centered at O, the intersection between the directions of the three actuated prismatic joints.
$\mathcal{R}_P(P,X,Y,Z)$: coordinate frame attached to the end-effector.
$\mathcal{R}_i(A_i,x_i,y_i,z_i)$: coordinate frame attached to the i^{th} prismatic joint, $i=1,2,3$.
$\mathbf{p} = \left[\, p_x\ p_y\ p_z \,\right]^T$: vector of the Cartesian coordinates of the end-effector, expressed in $\mathcal{R}_b$.
$\delta\mathbf{p} = \left[\, \delta p_x\ \delta p_y\ \delta p_z \,\right]^T$: position error of the end-effector, expressed in $\mathcal{R}_b$.
$\delta\theta = \left[\, \delta\theta_x\ \delta\theta_y\ \delta\theta_z \,\right]^T$: orientation error of the end-effector, expressed in $\mathcal{R}_b$.
ρ_i : displacement of the i^{th} prismatic joint.
$\delta\rho_i$: displacement error of the i^{th} prismatic joint.
L_i : theoretical length of the i^{th} parallelogram.
A_i, B_i, C_i : depicted in Fig. 1.
a_i : distance between points O and A_i.
r_i : distance between points P and C_i.
b_{1y}, b_{1z} : position errors of point B_1 along y and z axes, respectively.
b_{2x}, b_{2z} : position errors of point B_2 along x and z axes, respectively.
b_{3x}, b_{3y} : position errors of point B_3 along x and y axes, respectively.
$h_1 = b_{1y},\ k_1 = b_{1z},\ h_2 = b_{2x},\ k_2 = b_{2z},\ h_3 = b_{3x},\ k_3 = b_{3y}$.
d_i : nominal width of the i^{th} parallelogram.
δL_i : variation in the length of the i^{th} parallelogram.
δL_{ij} : variation in the length of link $\overline{B_{ij}C_{ij}}$, $j=1,2$ (see Fig. 2).
δb_i : variation in the length of link $\overline{B_{i1}B_{i2}}$.
δc_i : variation in the length of link $\overline{C_{i1}C_{i2}}$.
δl_i : parallelism error of links $\overline{B_{i1}B_{i2}}$ and $\overline{C_{i1}C_{i2}}$.
δm_i : parallelism error of links $\overline{B_{i1}C_{i1}}$ and $\overline{B_{i2}C_{i2}}$.
$\mathbf{w}_i$: direction of links $\overline{B_{i1}C_{i1}}$ and $\overline{B_{i2}C_{i2}}$.
$\delta\mathbf{w}_i$: variation in the direction of links $\overline{B_{i1}C_{i1}}$ and $\overline{B_{i2}C_{i2}}$.
$\delta\mathbf{e}_i$: sum of the position errors of points A_i, B_i, C_i.

*IRCCyN: UMR n° 6597 CNRS, École Centrale de Nantes, Université de Nantes, École des Mines de Nantes

$\delta\theta_{Ai} = \left[\, \delta\theta_{Aix}\ \delta\theta_{Aiy}\ \delta\theta_{Aiz} \,\right]^T$: angular variation in the direction of the i^{th} prismatic joint.

$\delta\theta_{Bi} = \left[\, \delta\theta_{Bix}\ \delta\theta_{Biy}\ \delta\theta_{Biz} \,\right]^T$: angular variation between $\overline{B_{i1}B_{i2}}$ and the direction of the i^{th} prismatic joint.

$\delta\theta_{Ci} = \left[\, \delta\theta_{Cix}\ \delta\theta_{Ciy}\ \delta\theta_{Ciz} \,\right]^T$: angular variation between the end-effector and $\overline{C_{i1}C_{i2}}$.

$\delta\gamma_i = \left[\, \delta\gamma_{ix}\ \delta\gamma_{iy}\ \delta\gamma_{iz} \,\right]^T$ sum of the orientation errors of the i^{th} parallelogram with respect to the i^{th} prismatic joint and the end-effector.

DOF : degree-of-freedom.

PKM : parallel kinematic machine.

1 Introduction

For two decades, parallel manipulators have attracted the attention of more and more researchers who consider them as valuable alternative design for robotic mechanisms. As stated by numerous authors, conventional serial kinematic machines have already reached their dynamic performance limits, which are bounded by high stiffness of the machine components required to support sequential joints, links and actuators. Thus, while having good operating characteristics (large workspace, high flexibility and manoeuvrability), serial manipulators have disadvantages of low stiffness and low power. Conversely, parallel kinematic machines (PKM) offer essential advantages over their serial counterparts (lower moving masses, higher stiffness and payload-to-weight ratio, higher natural frequencies, better accuracy, simpler modular mechanical construction, possibility to locate actuators on the fixed base).

However, PKM are not necessarily more accurate than their serial counterparts. Indeed, even if the dimensional variations can be compensated with PKM, they can also be amplified contrary to with their serial counterparts, [1]. Wang et al. [2] studied the effect of manufacturing tolerances on the accuracy of a Stewart platform. Kim et al. [3] used a forward error bound analysis to find the error bound of the end-effector of a Stewart platform when the error bounds of the joints are given, and an inverse error bound analysis to determine those of the joints for the given error bound of the end-effector. Kim and Tsai [4] studied the effect of misalignment of linear actuators of a 3-DOF translational parallel manipulator on the motion of its moving platform. Han et al. [5] used a kinematic sensitivity analysis method to explain the gross motions of a 3-UPU parallel mechanism, and they showed that it is highly sensitive to certain minute clearances. Fan et al. [6] analyzed the sensitivity of the 3-PRS parallel kinematic spindle platform of a serial-parallel machine tool. Verner et al. [7] presented a new method for optimal calibration of PKM based on the exploitation of the least error sensitive regions in their workspace and geometric parameters space. As a matter of fact, they used a Monte Carlo simulation to determine and map the sensitivities to geometric parameters. Moreover, Caro et al. [8] developed a tolerance synthesis method for mechanisms based on a robust design approach.

This paper aims at analyzing the sensitivity of the Orthoglide to its dimensional and angular variations. The Orthoglide is a three degree-of-freedom (DOF) translational PKM developed by Chablat and Wenger [9]. A small-scale prototype of this manipulator was built at IRCCyN.

Here, the sensitivity of the Orthoglide is studied by means of two complementary methods. First, a linkage kinematic analysis is used to have a rough idea of the influence of the dimensional variations to its end-effector and to show that the variations in design parameters of the same type from one leg to another have the same influence on the location of the end-effector. Although this method is compact, it cannot be used to know the influence of the variations in the parallelograms. Thus, a differential vector method is developed to study the influence of the dimensional and angular variations in the parts of the manipulator, and particularly variations in the parallelograms, on the position and the orientation of its end-effector.

In the isotropic kinematic configuration, the end-effector of the manipulator is located at the intersection between the directions of its three actuated prismatic joints, and the condition number of its kinematic Jacobian matrix is equal to one, [10]. It is shown that this configuration is the least sensitive one to geometrical variations, contrary to the closest configurations to its kinematic singular configurations, which are the most sensitive to geometrical variations.

Although the two sensitivity analysis methods are applied to a particular PKM, these methods can be readily applied to other 3-DOF Delta-linear PKM such as ones with parallel linear joints instead of orthogonal ones.

2 Manipulator Geometry

The kinematic architecture of the Orthoglide is shown in Fig.1. It consists of three identical parallel chains that are formally described as PRP$_a$RR, where P, R and P$_a$ denote the prismatic, revolute, and parallelogram joints respectively, as shown in Fig.2.

The mechanism input is made up of three actuated orthogonal prismatic joints. The output body (with a tool mounting flange) is connected to the prismatic joints through a set of three kinematic chains. Inside each chain, one parallelogram is used and oriented in a manner that the output body is restricted to translational movements only.

The small-scale prototype of the Orthoglide was designed to reach Cartesian velocity of 1.2 m/s and an acceleration of 17 m/s^2. The desired payload is 4 kg (spindle, tool, included). The size of its prescribed cubic workspace, C_u, is $200 \times 200 \times 200$ mm, where the velocity transmission factors are bounded between $1/2$ and 2. The three legs are supposed to be identical. According to [9], the nominal lengths, L_i, and widths, d_i, of the par-

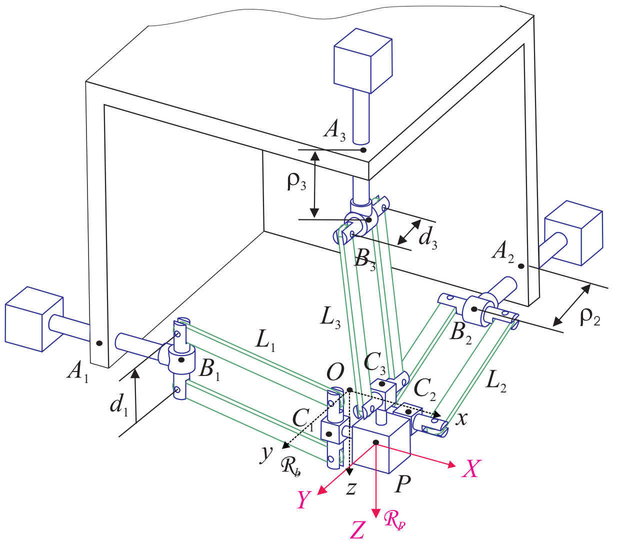

Figure 1. Basic kinematic architecture of the Orthoglide

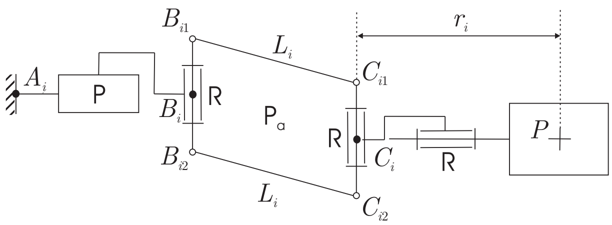

Figure 2. Morphology of the i^{th} leg of the Orthoglide

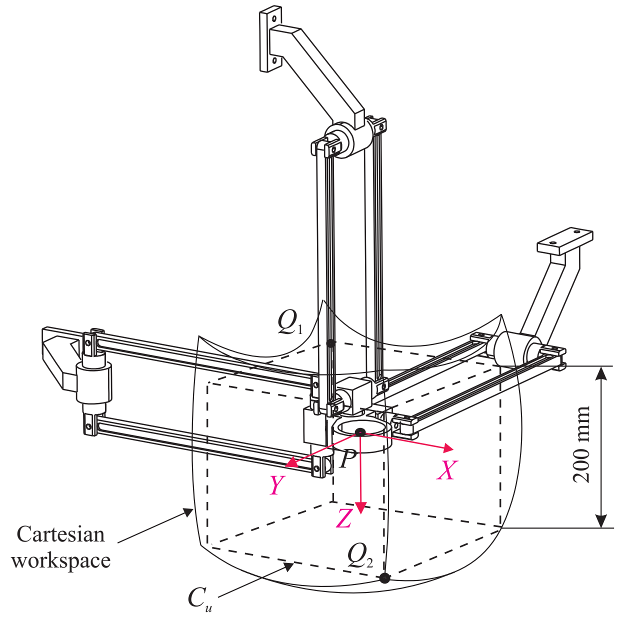

Figure 3. Cartesian workspace, C_u, points Q_1 and Q_2

allelograms, and the nominal distances, r_i, between points C_i and the end-effector P are identical, *i.e.*: $L = L_1 = L_2 = L_3 = 310.58$ mm, $d = d_1 = d_2 = d_3 = 80$ mm, $r = r_1 = r_2 = r_3 = 31$ mm.

As depicted in Fig.3, Q_1 and Q_2, vertices of C_u, are defined at the intersection between the Cartesian workspace boundary and the axis $x = y = z$ expressed in the reference coordinate frame $\mathcal{R}_b$. Q_1 and Q_2 are the closest points to the singularity surfaces. Their Cartesian coordinates, expressed in $\mathcal{R}_b$, are equal to (-73.21,-73.21,-73.21) and (126.79,126.79,126.79), respectively.

The parts of the manipulator are supposed to be rigid-bodies and there is no joint clearance. The legs of the manipulator, composed of one prismatic joint, one parallelogram, and three revolute joints, generate a five DOF motion each. Besides, they are identical. Therefore, according to Karouia et al. [11], the manipulator is isostatic. Thus, the results obtained by the sensitivity analysis methods developed in this paper are meaningful.

3 Sensitivity Analysis

Two complementary methods are used to study the sensitivity of the Orthoglide. First, a linkage kinematic analysis is used to have a rough idea of the influence of the dimensional variations to its end-effector. Although this method is compact, it cannot be used to know the influence of the variations in the parallelograms. Thus, a differential vector method is used to study the influence of the dimensional and angular variations in the parts of the manipulator, and particularly variations in the parallelograms, on the position and the orientation of its end-effector.

3.1 Linkage Kinematic Analysis

This method aims at computing the sensitivity coefficients of the position of the end-effector, P, to the design parameters of the manipulator. First, three implicit functions depicting the kinematic of the manipulator are obtained. A relation between the variations in the position of P and the variations in the design parameters follows from these functions. Finally a sensitivity matrix, which gathers the sensitivity coefficients of P, follows from the previous relation written in matrix form.

3.1.1 Formulation

Figure 1 depicts the design parameters taken into account. Points A_1, A_2, and A_3 are the bases of the prismatic joints. Their Cartesian coordinates, expressed in $\mathcal{R}_b$, are $\mathbf{a}_1$, $\mathbf{a}_2$, and $\mathbf{a}_3$, respectively.

$$\mathbf{a}_1 = \begin{bmatrix} -a_1 & 0 & 0 \end{bmatrix}^T \tag{1a}$$

$$\mathbf{a}_2 = \begin{bmatrix} 0 & -a_2 & 0 \end{bmatrix}^T \tag{1b}$$

$$\mathbf{a}_3 = \begin{bmatrix} 0 & 0 & -a_3 \end{bmatrix}^T \tag{1c}$$

where a_i is the distance between points A_i and O, the origin of $\mathcal{R}_b$. Points B_1, B_2 and B_3 are the links between the prismatic and parallelogram joints. Their Cartesian coordinates, expressed in $\mathcal{R}_b$ are:

$$\mathbf{b}_1 = \begin{bmatrix} -a_1 + \rho_1 \\ b_{1y} \\ b_{1z} \end{bmatrix} \tag{2a}$$

$$\mathbf{b}_2 = \begin{bmatrix} b_{2x} \\ -a_2 + \rho_2 \\ b_{2z} \end{bmatrix} \tag{2b}$$

$$\mathbf{b}_3 = \begin{bmatrix} b_{3x} \\ b_{3y} \\ -a_3 + \rho_3 \end{bmatrix} \tag{2c}$$

where ρ_i is the displacement of the i^{th} prismatic joint. b_{1y} and b_{1z} are the position errors of point B_1 according to y and z axes. b_{2x} and b_{2z} are the position errors of point B_2 according to x and z axes. b_{3x} and b_{3y} are the position errors of point B_3 according to x and y axes. These errors result from the orientation errors of the directions of the prismatic actuated joints. The Cartesian coordinates of C_1, C_2, and C_3, expressed in $\mathcal{R}_b$, are the following:

$$\mathbf{c}_1 = \begin{bmatrix} p_x - r_1 & 0 & 0 \end{bmatrix}^T \tag{3a}$$

$$\mathbf{c}_2 = \begin{bmatrix} 0 & p_y - r_2 & 0 \end{bmatrix}^T \tag{3b}$$

$$\mathbf{c}_3 = \begin{bmatrix} 0 & 0 & p_z - r_3 \end{bmatrix}^T \tag{3c}$$

where $\mathbf{p} = \begin{bmatrix} p_x & p_y & p_z \end{bmatrix}^T$ is the vector of the Cartesian coordinates of the end-effector P, expressed in $\mathcal{R}_b$.

The expressions of the nominal lengths of the parallelograms follow from eq.(4),

$$L_i = \|\mathbf{c}_i - \mathbf{b}_i\|_2 \ , \ i = 1,2,3 \tag{4}$$

where L_i is the nominal length of the i^{th} parallelogram and $\|.\|_2$ is the Euclidean norm. Three implicit functions follow from eq.(4) and are given by the following equations:

$$F_1 = (-r_1 + p_x + a_1 - \rho_1)^2 + (p_y - b_{1y})^2 + (p_z - b_{1z})^2 - L_1^2 = 0$$
$$F_2 = (p_x - b_{2x})^2 + (-r_2 + p_y + a_2 - \rho_2)^2 + (p_z - b_{2z})^2 - L_2^2 = 0$$
$$F_3 = (p_x - b_{3x})^2 + (p_y - b_{3y})^2 + (-r_3 + p_z + a_3 - \rho_3)^2 - L_3^2 = 0$$

By differentiating functions F_1, F_2, and F_3, with respect to the design parameters of the manipulator and the position of the end-effector, we obtain a relation between the positioning error of the end-effector, $\delta\mathbf{p}$, and the variations in the design parameters, $\delta\mathbf{q}_i$.

$$\delta F_i = \mathbf{A}_i \delta\mathbf{p} + \mathbf{B}_i \delta\mathbf{q}_i = 0 \ , \ i = 1,2,3 \tag{5}$$

with

$$\mathbf{A}_i = \begin{bmatrix} \partial F_i/\partial p_x & \partial F_i/\partial p_y & \partial F_i/\partial p_z \end{bmatrix} \tag{6}$$
$$\mathbf{B}_i = \begin{bmatrix} \partial F_i/\partial a_i & \partial F_i/\partial b_{iy} & \partial F_i/\partial b_{iz} & \partial F_i/\partial \rho_i & \partial F_i/\partial L_i & \partial F_i/\partial r_i \end{bmatrix} \tag{7}$$
$$\delta\mathbf{p} = \begin{bmatrix} \delta p_x & \delta p_y & \delta p_z \end{bmatrix}^T \tag{8}$$
$$\delta\mathbf{q}_i = \begin{bmatrix} \delta a_i & \delta h_i & \delta k_i & \delta\rho_i & \delta L_i & \delta r_i \end{bmatrix}^T \tag{9}$$

where δa_i, δh_i, δk_i, $\delta\rho_i$, δL_i, and δr_i, depict the variations in a_i, h_i, k_i, ρ_i, L_i, and r_i, respectively with $h_1 = b_{1y}$, $k_1 = b_{1z}$, $h_2 = b_{2x}$, $k_2 = b_{2z}$, $h_3 = b_{3x}$, $k_3 = b_{3y}$.

Integrating the three loops of eq.(5) together and separating the position parameters and design parameters to different sides yields the following simplified matrix form:

$$\mathbf{A}\delta\mathbf{p} + \mathbf{B}\delta\mathbf{q} = 0 \tag{10}$$

with

$$\mathbf{A} = \begin{bmatrix} \mathbf{A}_1^T \mathbf{A}_2^T \mathbf{A}_3^T \end{bmatrix}^T \in \mathbb{R}^{3\times 3} \tag{11}$$
$$\mathbf{B} = \begin{bmatrix} \mathbf{B}_1 & 0 & 0 \\ 0 & \mathbf{B}_2 & 0 \\ 0 & 0 & \mathbf{B}_3 \end{bmatrix} \in \mathbb{R}^{3\times 18} \tag{12}$$
$$\delta\mathbf{q} = \begin{bmatrix} \delta\mathbf{q}_1^T & \delta\mathbf{q}_2^T & \delta\mathbf{q}_3^T \end{bmatrix}^T \in \mathbb{R}^{18\times 1} \tag{13}$$

Equation (10) takes into account the coupling effect of the three independent structure loops. According to [9], $\mathbf{A}$ is the parallel Jacobian kinematic matrix of the Orthoglide, which does not meet parallel kinematic singularities when its end-effector covers C_u. Therefore, $\mathbf{A}$ is not singular and its inverse, $\mathbf{A}^{-1}$, exists. Thus, the positioning error of the end-effector can be computed using eq.(14).

$$\delta\mathbf{p} = \mathbf{C}\ \delta\mathbf{q} \tag{14}$$

where

$$\mathbf{C} = -\mathbf{A}^{-1}\mathbf{B} = \begin{bmatrix} \partial p_x/\partial a_1 & \partial p_x/\partial h_1 & \cdots & \partial p_x/\partial r_3 \\ \partial p_y/\partial a_1 & \partial p_y/\partial h_1 & \cdots & \partial p_y/\partial r_3 \\ \partial p_z/\partial a_1 & \partial p_z/\partial h_1 & \cdots & \partial p_z/\partial r_3 \end{bmatrix} \in \mathbb{R}^{3\times 18} \tag{15}$$

represents the sensitivity matrix of the manipulator. The terms of $\mathbf{C}$ are the sensitivity coefficients of the Cartesian coordinates of the end-effector to the design parameters and are used to analyze the sensitivity of the Orthoglide.

3.1.2 Results of the Linkage Kinematic Analysis

The sensitivity matrix **C** of the manipulator depends on the position of its end-effector.

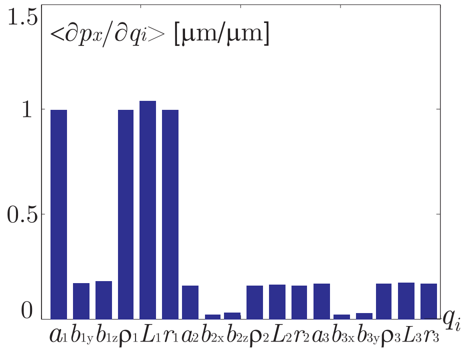

Figure 4. Mean of sensitivity of p_x throughout C_u

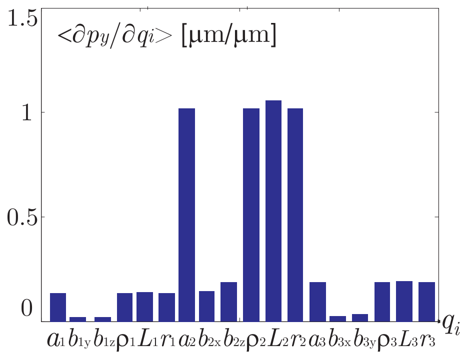

Figure 5. Mean of sensitivity of p_y throughout C_u

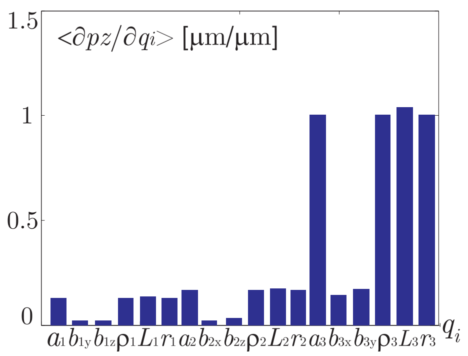

Figure 6. Mean of sensitivity of p_z throughout C_u

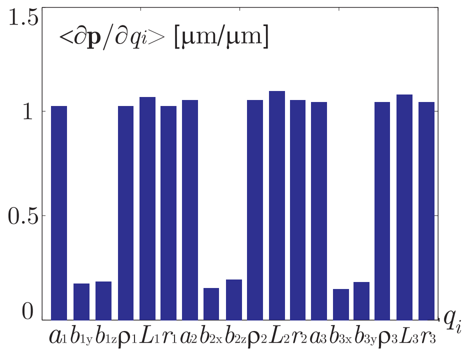

Figure 7. Mean of sensitivity of **p** throughout C_u

Figures 4, 5, 6 and 7 depict the mean of the sensitivity coefficients of p_x, p_y, p_z, and **p**, when the end-effector covers C_u. It appears that the position of the end-effector is very sensitive to variations in the position of points A_i, variations in the lengths of the parallelograms, L_i, variations in the lengths of prismatic joints, ρ_i, and variations in the position of points C_i defined by r_i (see Fig.2). However, it is little sensitive to the orientation errors of the direction of the prismatic joints, defined by parameters $b_{1y}, b_{1z}, b_{2x}, b_{2z}, b_{3x}, b_{3y}$. Besides, it is noteworthy that p_x (p_y , p_z, respectively) is very sensitive to the design parameters which make up the 1^{st} (2^{nd}, 3^{rd}, respectively) leg of the manipulator, contrary to the others. That is due to the symmetry of the architecture of the manipulator. Henceforth, only the variations in the design parameters of the first leg of the manipulator will be taken into account. Indeed, the sensitivity of the position of the end-effector to the variations in the design parameters of the second and the third legs of the manipulator can be deduced from the sensitivity of the position of the end-effector to variations in the design parameters of the first leg.

Chablat et al. [9] showed that if the prescribed bounds of the velocity transmission factors (the kinematic criteria used to dimension the manipulator) are satisfied at Q_1 and Q_2, then these bounds are satisfied throughout the prescribed cubic Cartesian workspace C_u. Q_1 and Q_2 are then the most critical points of C_u, whereas O is the most interesting point because it corresponds to the isotropic kinematic configuration of the manipulator. Here, we assume that if the prescribed bounds of the sensitivity coefficients are satisfied at Q_1 and Q_2, then these bounds are satisfied throughout C_u.

Figures 8 and 9 depict the sensitivity coefficients of p_x and p_y to the dimensional variations in the 1^{st} leg, *i.e.*: $a_1, b_{1y}, b_{1z}, \rho_1, L_1, r_1$, along Q_1Q_2. It appears that these coefficients are a minimum in the isotropic configuration, *i.e.*: $P \equiv O$, and a maximum when $P \equiv Q_2$, *i.e.*: in the closest configuration to the singular one. Figure 10 depicts the sensitivity coefficients of **p** along diagonal Q_1Q_2. It is noteworthy that all the sensitivity coefficients are a minimum when $P \equiv O$ and a maximum when

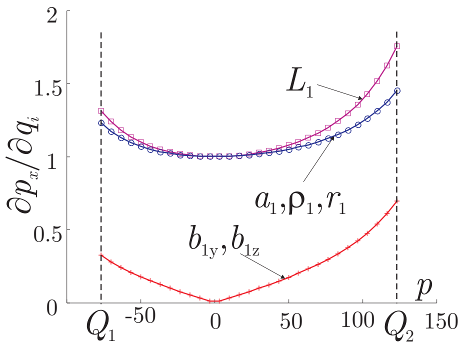

Figure 8. Sensitivity of p_x to the variations in the 1^{st} leg

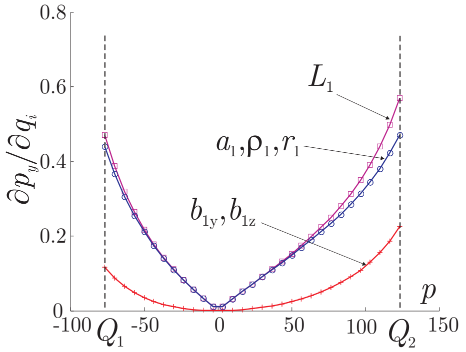

Figure 9. Sensitivity of p_y to the variations in the 1^{st} leg

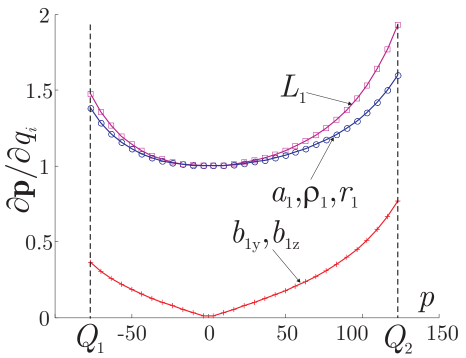

Figure 10. Sensitivity of $\mathbf{p}$ to the variations in the 1^{st} leg

$P \equiv Q_2$. Finally, figure 11 depicts the global sensitivities of $\mathbf{p}$, p_x, p_y, and p_z to the dimensional variations. It appears that they are a minimum when $P \equiv O$, and a maximum when $P \equiv Q_2$.

Figures 12 and 13 depict the sensitivity coefficients of p_x and $\mathbf{p}$ in the isotropic configuration. In this configuration, the position error of the end-effector does not depend on the orientation errors of the directions of the prismatic joints because the sensitivity of the position of P to variations in $b_{1y}, b_{1z}, b_{2x}, b_{2z}, b_{3x}, b_{3y}$ is null in this configuration. Besides, variations in p_x, p_y, and

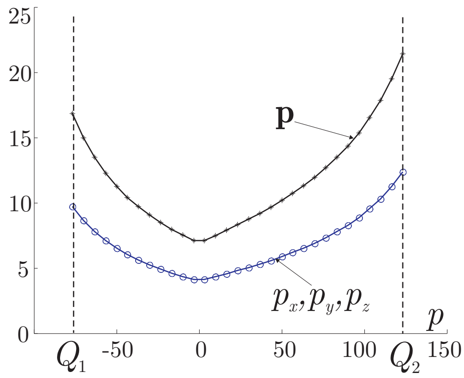

Figure 11. Global sensitivity of $\mathbf{p}$, p_x, p_y, and p_z

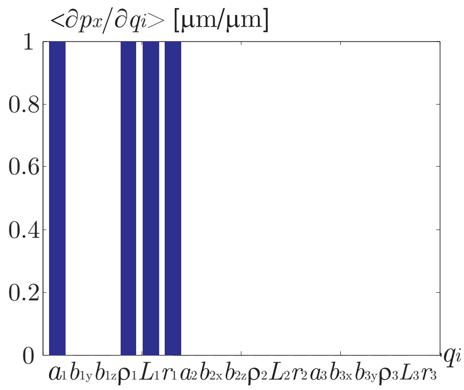

Figure 12. Sensitivity of p_x in the isotropic configuration

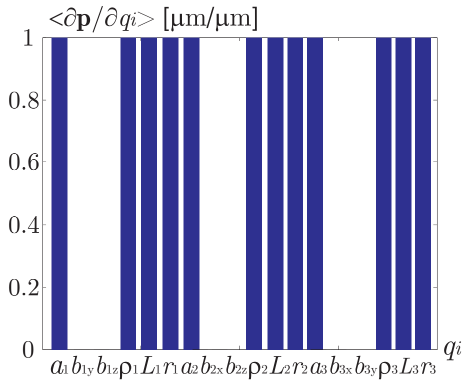

Figure 13. Sensitivity of $\mathbf{p}$ in the isotropic configuration

p_z are decoupled in this configuration. Indeed, variarions in p_x, (p_y, p_z, respectively) are only due to dimensional variations in the 1^{st}, (2^{nd}, 3^{rd}, respectively) leg of the manipulator. The corresponding sensitivity coefficients are equal to 1. It means that the dimensional variations are neither amplified nor compensated in the isotropic configuration.

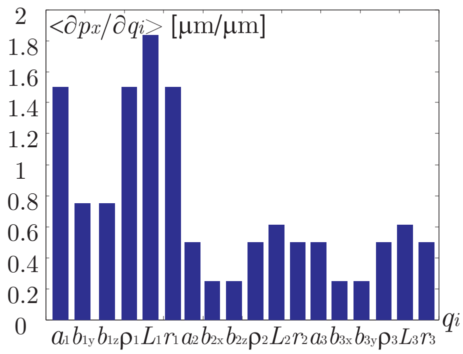

Figure 14. Q_2 configuration, sensitivity of p_x

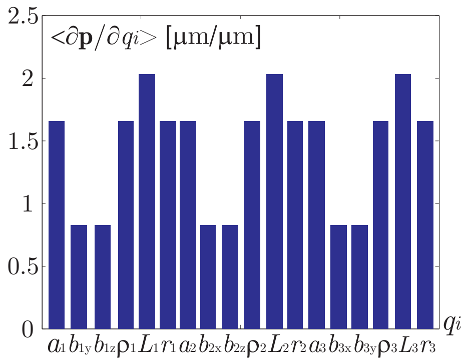

Figure 15. Q_2 configuration, sensitivity of $\mathbf{p}$

Figures 14 and 15 depict the sensitivity coefficients of p_x and $\mathbf{p}$ when the end-effector hits Q_2 ($P \equiv Q_2$). In this case, variations in p_x, p_y, and p_z are coupled. For example, variations in p_x are due to both dimensional variations in the 1^{st} leg and variations in the 2^{nd} and the 3^{rd} legs. Besides, the amplification of the dimensional variations is important. Indeed, the sensitivity coefficients of $\mathbf{p}$ are close to 2 in this configuration. For example, as the sensitivity coefficient relating to L_1 is equal to 1.9, the position error of the end-effector will be equal to $19\mu m$ if $\delta L_1 = 10\mu m$. Moreover, we noticed numerically that Q_2 configuration is the most sensitive configuration to dimensional variations of the manipulator.

According to figures 4 - 7, 12 - 15, variations in design parameters of the same type from one leg to another have the same influence on the location of the end-effector.

However, this linkage kinematic method does not take into account variations in the parallelograms, except the variations in their global length. Thus, a differential vector method is developed below.

3.2 Differential Vector Method

In this section, we perfect a sensitivity analysis method of the Orthoglide, which complements the previous one. This method is used to analyze the sensitivity of the position and the orientation of the end-effector to dimensional and angular variations, and particularly to the variations in the parallelograms. Moreover, it allows us to distinguish the variations which are responsible for the position errors of the end-effector from the ones which are responsible for its orientation errors. To develop this method, we were inspired by a Huang & al. work on a parallel kinematic machine, which is made up of parallelogram joints too [12].

First, we express the dimensional and angular variations in vectorial form. Then, a relation between the position and the orientation errors of the end-effector is obtained from the closed-loop kinematic equations. The expressions of the orientation and the position errors of the end-effector, with respect to the variations in the design parameters, are deduced from this relation. Finally, we introduce two sensitivity indices to assess the sensitivity of the position and the orientation of the end-effector to dimensional and angular variations, and particularly to the parallelism errors of the bars of the parallelograms.

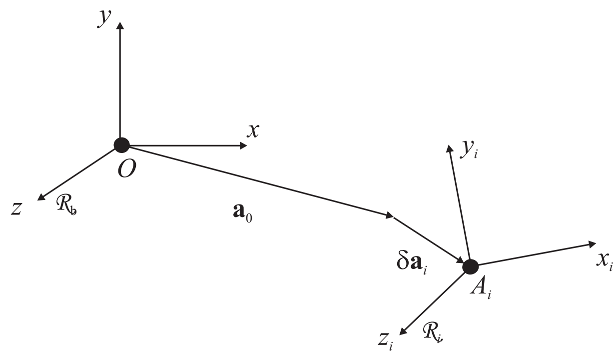

Figure 16. Variations in $O - A_i$ chain

3.2.1 Formulation

The schematic drawing of the i^{th} leg of the Orthoglide depicted in Fig.2 is split in order to depict the variations in design parameters in a vectoriel form. The closed-loop kinematic chains $O - A_i - B_i - B_{ij} - C_{ij} - C_i - P$, $i = 1,2,3$, $j = 1,2$, are depicted by Figs.16-19. $\mathcal{R}_i$ is the coordinate frame attached to the i^{th} prismatic joint. $\mathbf{o}, \mathbf{a}_i, \mathbf{b}_i, \mathbf{b}_{ij}, \mathbf{c}_{ij}, \mathbf{c}_i, \mathbf{p}$, are the Cartesian coordinates of points $O, A_i, B_i, B_{ij}, C_{ij}, C_i, P$, respectively, expressed in $\mathcal{R}_i$ and depicted in Fig.2.

According to Fig.16,

$$\mathbf{a}_i - \mathbf{o} = \mathbf{R}_i(\mathbf{a}_0 + \delta\mathbf{a}_i) \tag{16}$$

where $\mathbf{a}_0$ is the nominal position vector of A_i with respect to O expressed in $\mathcal{R}_i$, $\delta\mathbf{a}_i$ is the positioning error of A_i. $\mathbf{R}_i$ is the transformation matrix from $\mathcal{R}_i$ to $\mathcal{R}_b$. $\mathbf{I}_3$ is the (3×3) identity matrix and

$$\mathbf{R}_1 = \mathbf{I}_3 \tag{17}$$

$$\mathbf{R}_2 = \begin{bmatrix} 0 & 0 & -1 \\ 1 & 0 & 0 \\ 0 & -1 & 0 \end{bmatrix} \tag{18}$$

$$\mathbf{R}_3 = \begin{bmatrix} 0 & 1 & 0 \\ 0 & 0 & 1 \\ 1 & 0 & 0 \end{bmatrix} \tag{19}$$

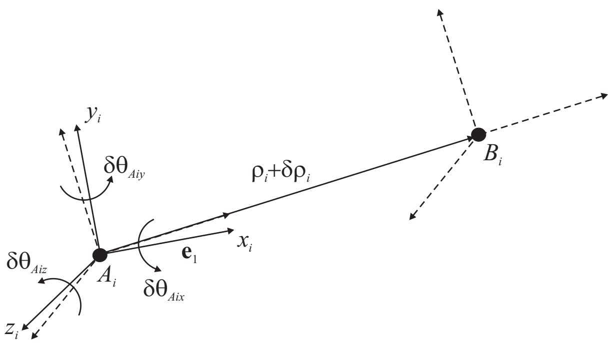

Figure 17. Variations in $A_i - B_i$ chain

According to Fig.17,

$$\mathbf{b}_i - \mathbf{a}_i = \mathbf{R}_i(\rho_i + \delta\rho_i)\mathbf{e}_1 + \mathbf{R}_i\delta\theta_{Ai} \times (\rho_i + \delta\rho_i)\mathbf{e}_1 \tag{20}$$

where ρ_i is the displacement of the i^{th} prismatic joint, $\delta\rho_i$ is its displacement error, $\delta\theta_{Ai} = \begin{bmatrix} \delta\theta_{Aix} & \delta\theta_{Aiy} & \delta\theta_{Aiz} \end{bmatrix}^T$ is the angular variation of its direction, and

$$\mathbf{e}_1 = \begin{bmatrix} 1 \\ 0 \\ 0 \end{bmatrix} \tag{21}$$

$$\mathbf{e}_2 = \begin{bmatrix} 0 \\ 0 \\ 1 \end{bmatrix} \tag{22}$$

$$\xi(j) = \begin{cases} 1 & \text{if } j = 1 \\ -1 & \text{if } j = 2 \end{cases} \tag{23}$$

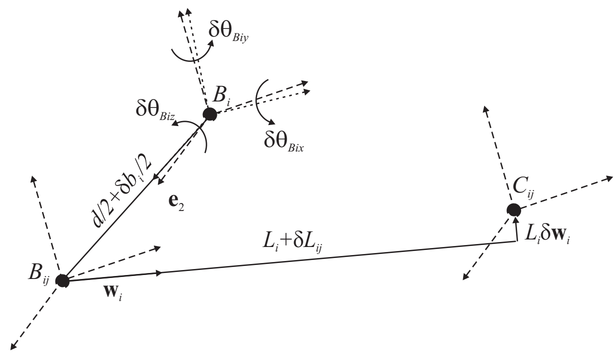

Figure 18. Variations in $B_i - B_{ij} - C_{ij}$ chain

According to Fig.18,

$$\begin{aligned} \mathbf{b}_{ij} - \mathbf{b}_i &= \mathbf{R}_i[\mathbf{I}_3 + \delta\theta_{Ai}\times]\big(\xi(j)(d/2 + \delta b_i/2) \\ &\quad [\mathbf{I}_3 + \delta\theta_{Bi}\times]\mathbf{e}_2\big) \end{aligned} \tag{24}$$

$$\mathbf{c}_{ij} - \mathbf{b}_{ij} = L_i\mathbf{w}_i + \delta L_{ij}\mathbf{w}_i + L_i\delta\mathbf{w}_i \tag{25}$$

where d is the nominal width of the parallelogram, δb_i is the variation in the length of link $\overline{B_{i1}B_{i2}}$ and is supposed to be equally shared by each side of B_i. $\delta\theta_{Bi} = \begin{bmatrix} \delta\theta_{Bix} & \delta\theta_{Biy} & \delta\theta_{Biz} \end{bmatrix}^T$ is the orientation error of link $\overline{B_{i1}B_{i2}}$ with respect to the direction of the i^{th} prismatic joint, L_i is the length of the i^{th} parallelogram, δL_{ij} is the variation in the length of link $\overline{B_{ij}C_{ij}}$, of which $\mathbf{w}_i$ is the direction, and $\delta\mathbf{w}_i$ is the variation in this direction, orthogonal to $\mathbf{w}_i$.

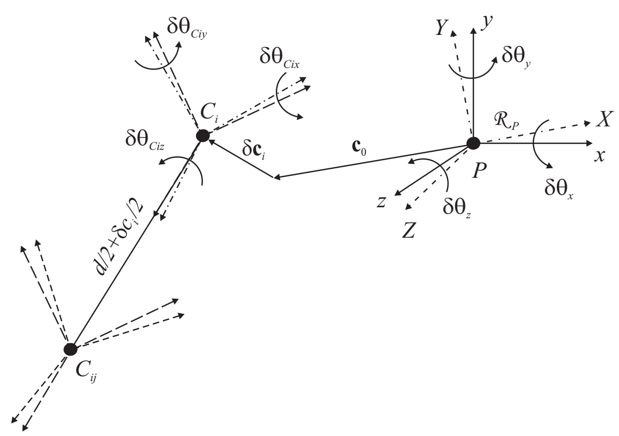

Figure 19. Variations in $C_{ij} - C_i - P$ chain

According to Fig.19,

$$\mathbf{c}_{ij} - \mathbf{c}_i = \mathbf{R}_i[\mathbf{I}_3 + \delta\theta\times]\big(\xi(j)(d/2+\delta c_i/2)\, [\mathbf{I}_3 + \delta\theta_{Ci}\times]\mathbf{e}_2\big) \quad (26)$$

$$\mathbf{c}_i - \mathbf{p} = [\mathbf{I}_3 + \delta\theta\times]\mathbf{R}_i(\mathbf{c}_0 + \delta\mathbf{c}_i) \quad (27)$$

where δc_i is the variation in the length of link $\overline{C_{i1}C_{i2}}$, which is supposed to be equally shared by each side of C_i. $\delta\theta_{Ci} = \begin{bmatrix} \delta\theta_{Cix} & \delta\theta_{Ciy} & \delta\theta_{Ciz} \end{bmatrix}^T$ is the orientation error of link $\overline{C_{i1}C_{i2}}$ with respect to link $\overline{C_iP}$. $\mathbf{c}_0$ is the nominal position vector of C_i with respect to end-effector P, expressed in $\mathcal{R}_i$, $\delta\mathbf{c}_i$ is the position error of C_i expressed in $\mathcal{R}_i$, and $\delta\theta = \begin{bmatrix} \delta\theta_x & \delta\theta_y & \delta\theta_z \end{bmatrix}^T$ is the orientation error of the end-effector, expressed in $\mathcal{R}_b$.

Implementing linearization of eqs.(16-26) and removing the components associated with the nominal constrained equation $\mathbf{p}_0 = \mathbf{R}_i(\mathbf{a}_0 + \rho_i\mathbf{e}_1 - \mathbf{c}_0) + L_i\mathbf{w}_i$, yields

$$\begin{aligned}\delta\mathbf{p} &= \mathbf{p} - \mathbf{p}_0 \\ &= \mathbf{R}_i\big(\delta\mathbf{e}_i + \rho_i(\delta\theta_{Ai}\times\mathbf{e}_1) + \xi(j)\; d/2\; (\delta\theta_{Ai}\times\mathbf{e}_2) + \\ &\quad \xi(j)\; d/2\; (\delta\gamma_i\times\mathbf{e}_2) + \xi(j)\; \delta m_i/2\; \mathbf{e}_2\big) + \\ &\quad \delta L_{ij}\mathbf{w}_i + L_i\delta\mathbf{w}_i - \delta\theta\times\mathbf{R}_i\big(\mathbf{c}_0 + d/2\,\xi(j)\;\mathbf{e}_2\big)\end{aligned} \quad (28)$$

where

- $\delta\mathbf{p}$ is the position error of the end-effector of the manipulator.
- $\delta\mathbf{e}_i = \delta\mathbf{a}_i + \delta\rho_i\mathbf{e}_1 - \delta\mathbf{c}_i$ is the sum of the position errors of points A_i, B_i, and C_i expressed in $\mathcal{R}_i$.
- $\delta\gamma_i = \delta\theta_{Bi} - \delta\theta_{Ci}$ is the sum of the orientation errors of the i^{th} parallelogram with respect to the i^{th} prismatic joint and the end-effector.
- $\delta m_i = \delta b_i - \delta c_i$ corresponds to the parallelism error of links $\overline{B_{i1}C_{i1}}$ and $\overline{B_{i2}C_{i2}}$, which is depicted by Fig.20.

Equation (28) shows the coupling of the position and orientation errors of the end-effector. Contrary to the orientation error, the position error can be compensated because the manipulator is a translational 3-DOF PKM. Thus, it is more important to minimize the geometrical variations, which are responsible for the orientation errors of the end-effector than the ones, which are responsible for its position errors.

The following equation is obtained by multiplying both sides of eq.(28) by $\mathbf{w}_i^T$ and utilizing the circularity of hybrid product.

$$\begin{aligned}\mathbf{w}_i^T\delta\mathbf{p} &= \mathbf{w}_i^T\mathbf{R}_i\delta\mathbf{e}_i + \rho_i(\mathbf{R}_i\mathbf{e}_1\times\mathbf{w}_i)^T\mathbf{R}_i\delta\theta_{Ai} + \xi(j)\; d/2 \\ &\quad (\mathbf{R}_i\mathbf{e}_2\times\mathbf{w}_i)^T\mathbf{R}_i(\delta\theta_{Ai}+\delta\gamma_i) + \xi(j)\;\delta m_i/2\;\mathbf{w}_i^T\mathbf{R}_i\mathbf{e}_2 \\ &\quad +\delta L_{ij} - \big(\mathbf{R}_i(\mathbf{c}_0 + \xi(j)\; d/2\;\mathbf{e}_2)\times\mathbf{w}_i\big)^T\delta\theta\end{aligned} \quad (29)$$

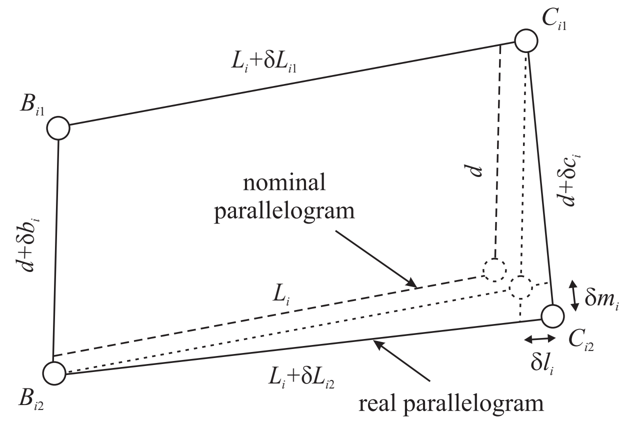

Figure 20. Variations in the i^{th} parallelogram

Orientation Error Mapping Function: By substraction of eqs.(29) written for $j=1$ and $j=2$, and for the i^{th} kinematic chain, a relation is obtained between the orientation error of the end-effector and the variations in design parameters, which is independent of the position error of the end-effector.

$$d(\mathbf{R}_i\mathbf{e}_2\times\mathbf{w}_i)^T\delta\theta = \delta l_i + d(\mathbf{R}_i\mathbf{e}_2\times\mathbf{w}_i)^T\mathbf{R}_i(\delta\theta_{Ai}+\delta\gamma_i) + \delta m_i\;\mathbf{w}_i^T\mathbf{R}_i\mathbf{e}_2 \quad (30)$$

where $\delta l_i = \delta L_{i1} - \delta L_{i2}$, the relative length error of links $\overline{B_{i1}C_{i1}}$ and $\overline{B_{i2}C_{i2}}$, depicts the parallelism error of links $\overline{B_{i1}B_{i2}}$ and $\overline{C_{i1}C_{i2}}$ as shown in Fig.20. Equation (30) can be written in matrix form:

$$\delta\theta = \mathbf{J}_{\theta\theta}\varepsilon_\theta \quad (31)$$

with

$$\mathbf{J}_{\theta\theta} = \mathbf{D}^{-1}\mathbf{E} \quad (32)$$

$$\mathbf{D} = d\begin{bmatrix}(\mathbf{R}_1\mathbf{e}_2\times\mathbf{w}_1)^T \\ (\mathbf{R}_2\mathbf{e}_2\times\mathbf{w}_2)^T \\ (\mathbf{R}_3\mathbf{e}_2\times\mathbf{w}_3)^T\end{bmatrix} \quad (33)$$

$$\mathbf{E} = \begin{bmatrix}\mathbf{E}_1 & \cdots & \cdots \\ \cdots & \mathbf{E}_2 & \cdots \\ \cdots & \cdots & \mathbf{E}_3\end{bmatrix} \quad (34)$$

$$\mathbf{E}_i = \begin{bmatrix}1 & \mathbf{w}_i^T\mathbf{R}_i\mathbf{e}_2 & d(\mathbf{R}_i\mathbf{e}_2\times\mathbf{w}_i)^T\mathbf{R}_i & d(\mathbf{R}_i\mathbf{e}_2\times\mathbf{w}_i)^T\mathbf{R}_i\end{bmatrix} \quad (35)$$

$\delta\theta$ is the orientation error of the end-effector expressed in $\mathcal{R}_b$, and $\varepsilon_\theta = (\varepsilon_{\theta1}^T, \varepsilon_{\theta2}^T, \varepsilon_{\theta3}^T)^T$ such that $\varepsilon_{\theta i} = (\delta l_i, \delta m_i, \delta\theta_{Ai}^T, \delta\gamma_i^T)^T$. The determinant of $\mathbf{D}$ will be null if the normal vectors to the plans, which contain the three parallelograms respectively, are collinear, or if one parallelogram is flat. Here, this determinant is not null when P covers C_u because of the geometry of the manipulator. Therefore, $\mathbf{D}$ is nonsingular and its inverse $\mathbf{D}^{-1}$ exists.

As $(\mathbf{R}_i\mathbf{e}_2 \times \mathbf{w}_i)^T \perp \mathbf{R}_i\mathbf{e}_2$, $\delta\theta_{Aiz}$ and $\delta\gamma_{iz}$, the third components of $\delta\theta_{Ai}$ and $\delta\gamma_i$ expressed in $\mathcal{R}_i$, have no effect on the orientation of the end-effector. Thus, matrix $\mathbf{J}_{\theta\theta}$ can be simplified by eliminating its columns associated with $\delta\theta_{Aiz}$ and $\delta\gamma_{iz}$, $i = 1,2,3$. Finally, eighteen variations: δl_i, δm_i, $\delta\theta_{Aix}$, $\delta\theta_{Aiy}$, $\delta\gamma_{ix}$, $\delta\gamma_{iy}$, $i = 1,2,3$, should be responsible for the orientation error of the end-effector.

Position Error Mapping Function: By addition of eqs.(29) written for $j = 1$ and $j = 2$, and for the i^{th} kinematic chain, a relation is obtained between the position error of the end-effector and the variations in design parameters, which does not depend on $\delta\gamma_i$.

$$\mathbf{w}_i^T \delta\mathbf{p} = \delta L_i + \mathbf{w}_i^T \mathbf{R}_i \delta\mathbf{e}_i + \rho_i (\mathbf{R}_i\mathbf{e}_1 \times \mathbf{w}_i)^T \mathbf{R}_i \delta\theta_{Ai} - (\mathbf{R}_i\mathbf{c}_0 \times \mathbf{w}_i)^T \delta\theta \tag{36}$$

Equation (36) can be written in matrix form:

$$\delta\mathbf{p} = \mathbf{J}_{pp}\varepsilon_p + \mathbf{J}_{p\theta}\varepsilon_\theta = [\mathbf{J}_{pp}\mathbf{J}_{p\theta}] \begin{bmatrix} \varepsilon_p \\ \varepsilon_\theta \end{bmatrix} \tag{37}$$

with

$$\mathbf{J}_{pp} = \mathbf{F}^{-1}\mathbf{G} \tag{38}$$
$$\mathbf{J}_{p\theta} = \mathbf{F}^{-1}\mathbf{H}\mathbf{J}_{\theta\theta} \tag{39}$$
$$\mathbf{F} = [\mathbf{w}_1\mathbf{w}_2\mathbf{w}_3]^T \tag{40}$$
$$\mathbf{G} = \mathrm{diag}(\mathbf{G}_i) \tag{41}$$
$$\mathbf{G}_i = \left[\, 1 \;\; \mathbf{w}_i^T\mathbf{R}_i \;\; \rho_i(\mathbf{R}_i\mathbf{e}_1 \times \mathbf{w}_i)^T\mathbf{R}_i \,\right] \tag{42}$$
$$\mathbf{H} = -\left[\, \mathbf{R}_1\mathbf{c}_0 \times \mathbf{w}_1 \;\; \mathbf{R}_2\mathbf{c}_0 \times \mathbf{w}_2 \;\; \mathbf{R}_3\mathbf{c}_0 \times \mathbf{w}_3 \,\right] \tag{43}$$
$$\varepsilon_p = (\varepsilon_{p1}^T, \varepsilon_{p2}^T, \varepsilon_{p3}^T)^T \tag{44}$$
$$\varepsilon_{pi} = (\delta L_i, \delta\mathbf{e}_i^T, \delta\theta_{Ai}^T)^T \tag{45}$$

$\delta L_i = (\delta L_{i1} + \delta L_{i2})/2$ is the mean value of the variations in links $\overline{B_{i1}C_{i1}}$ and $\overline{B_{i2}C_{i2}}$, *i.e.*: the variation in the length of the i^{th} parallelogram. ε_p is the set of the variations in design parameters, which should be responsible for the position errors of the end-effector, except the ones which should be responsible for its orientation errors, *i.e.*: ε_θ. ε_p is made up of three kinds of errors: the variation in the length of the i^{th} parallelogram, *i.e.*: $\delta L_i, i = 1,2,3$, the position errors of points A_i, B_i, and C_i, *i.e.*: $\delta\mathbf{e}_i, i = 1,2,3$, and the orientation errors of the directions of the prismatic joints, *i.e.*: $\delta\theta_{Ai}$, $i = 1,2,3$. Besides, $\mathbf{F}$ is nonsingular and its inverse $\mathbf{F}^{-1}$ exists because $\mathbf{F}$ corresponds to the Jacobian kinematic matrix of the manipulator, which is not singular when P covers C_u, [9].

According to eq.(36) and as $(\mathbf{R}_i\mathbf{e}_1 \times \mathbf{w}_i)^T \perp \mathbf{R}_i\mathbf{e}_1$, matrix $\mathbf{J}_{pp}$ can be simplified by eliminating its columns associated with $\delta\theta_{Aix}$, $i = 1,2,3$. Finally, thirty-three variations: δL_i, δe_{ix}, δe_{iy}, δe_{iz}, $\delta\theta_{Aix}$, $\delta\theta_{Aiy}$, $\delta\theta_{Aiz}$, δl_i, δm_i, $\delta\gamma_{ix}$, $\delta\gamma_{iy}$, $i = 1,2,3$, should be responsible for the position error of the end-effector.

Rearranging matices $\mathbf{J}_{pp}$ and $\mathbf{J}_{p\theta}$, the position error of the end-effector can be expressed as:

$$\delta\mathbf{p} = \mathbf{J}\,\varepsilon_q = \left[\,\mathbf{J}_1 \;\mathbf{J}_2\; \mathbf{J}_3\,\right] (\varepsilon_{q1}\;\varepsilon_{q2}\;\varepsilon_{q3})^T \tag{46}$$

with $\varepsilon_{qi} = \left(\delta L_i, \delta e_{ix}, \delta e_{iy}, \delta e_{iz}, \delta\theta_{Aix}, \delta\theta_{Aiy}, \delta\theta_{Aiz}, \delta l_i, \delta m_i, \delta\gamma_{ix}, \delta\gamma_{iy}\right)$, and $\mathbf{J} \in \mathbb{R}^{3\times 33}$.

Sensitivity Indices: In order to investigate the influence of the design parameters errors on the position and the orientation of the end-effector, sensitivity indices are required. According to section 3.1.2, variations in the design parameters of the same type from one leg to the other have the same influence on the location of the end-effector. Thus, assuming that variations in the design parameters are independent, the sensitivity of the position of the end-effector to the variations in the k^{th} design parameter responsible for its position error, *i.e.*: $\varepsilon_{q(1,2,3)k}$, is called μ_k and is defined by eq.(47).

$$\mu_k = \sqrt{\sum_{i=1}^{3}\sum_{m=1}^{3} J_{imk}^2}\,,\; k = 1,\cdots,11 \tag{47}$$

Likewise, ν_r is a sensitivity index of the orientation of the end-effector to the variations in the r^{th} design parameter responsible for its orientation error, *i.e.*: $\varepsilon_{\theta(1,2,3)r}$. ν_r follows from eq.(31) and is defined by eq.(48).

$$\nu_r = \arccos\frac{\mathrm{tr}(\mathbf{Q}_r) - 1}{2} \tag{48}$$

where $\mathbf{Q}_r$ is the rotation matrix corresponding to the orientation error of the end-effector, and ν_r is a linear invariant: its global rotation [13].

$$\mathbf{Q}_r = \begin{bmatrix} C_{\nu_{zr}}C_{\nu_{yr}} & \left(C_{\nu_{zr}}S_{\nu_{yr}}S_{\nu_{xr}} - S_{\nu_{zr}}C_{\nu_{xr}}\right) & \left(C_{\nu_{zr}}S_{\nu_{yr}}C_{\nu_{xr}} + S_{\nu_{zr}}S_{\nu_{xr}}\right) \\ S_{\nu_{zr}}C_{\nu_{yr}} & \left(S_{\nu_{zr}}S_{\nu_{yr}}S_{\nu_{xr}} + C_{\nu_{zr}}C_{\nu_{xr}}\right) & \left(S_{\nu_{zr}}S_{\nu_{yr}}C_{\nu_{xr}} - C_{\nu_{zr}}S_{\nu_{xr}}\right) \\ -S_{\nu_{yr}} & C_{\nu_{yr}}S_{\nu_{xr}} & C_{\nu_{yr}}C_{\nu_{xr}} \end{bmatrix} \tag{49}$$

such that $C_{\nu_{xr}} = \cos\nu_{xr}$, $S_{\nu_{xr}} = \sin\nu_{xr}$, $C_{\nu_{yr}} = \cos\nu_{yr}$, $S_{\nu_{yr}} = \sin\nu_{yr}$, $C_{\nu_{zr}} = \cos\nu_{zr}$, $S_{\nu_{zr}} = \sin\nu_{zr}$, and

$$\nu_{xr} = \sqrt{\sum_{j=0}^{2} J^2_{\theta\theta 1(6j+r)}} \;,\; r = 1, \cdots, 6 \tag{50}$$

$$\nu_{yr} = \sqrt{\sum_{j=0}^{2} J^2_{\theta\theta 2(6j+r)}} \;,\; r = 1, \cdots, 6 \tag{51}$$

$$\nu_{zr} = \sqrt{\sum_{j=0}^{2} J^2_{\theta\theta 3(6j+r)}} \;,\; r = 1, \cdots, 6 \tag{52}$$

Finally, μ_k can be employed as a sensitivity index of the position of the end-effector to the k^{th} design parameter responsible for the position error. Likewise, ν_r can be employed as a sensitivity index of the orientation of the end-effector to the r^{th} design parameter responsible for the orientation error. It is noteworthy that these sensitivity indices depend on the location of the end-effector.

3.2.2 Results of the Differential Vector Method

The sensitivity indices defined by eqs.(47) and (48) are used to evaluate the sensitivity of the position and orientation of the end-effector to variations in design parameters, particularly to variations in the parallelograms.

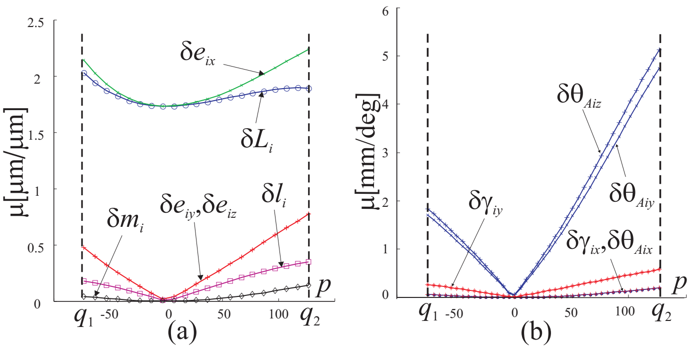

Figure 21. Sensitivity of the position of the end-effector along Q_1Q_2, (a): to dimensional variations, (b): to angular variations

Figures 21(a-b) depict the sensitivity of the position of the end-effector along the diagonal Q_1Q_2 of C_u, to dimensional variations and angular variations, respectively. According to Fig.21(a), the position of the end-effector is very sensitive to variations in the lengths of the parallelograms, δL_i, and to the position errors of points A_i, B_i, and C_i along axis x_i of $\mathcal{R}_i$, *i.e*: δe_{ix}. Conversely, the influence of δl_i and δm_i, the parallelism errors of the parallelograms, is low and even negligible in the kinematic isotropic configuration. According to Fig.21(b), the orientation errors of the prismatic joints depicted by $\delta\theta_{Aiy}$ and $\delta\theta_{Aiz}$ are the most influential angular errors on the position of the end-effector. Besides, the position of the end-effector is not sensitive to angular variations in the isotropic configuration.

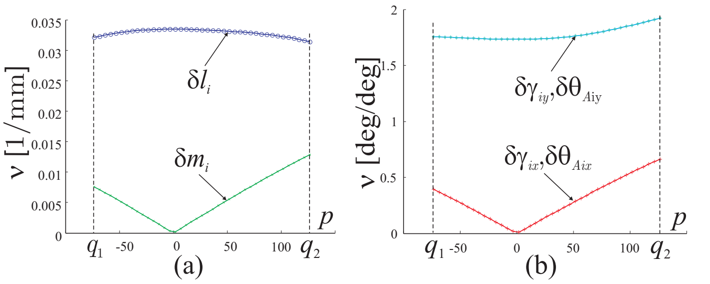

Figure 22. Sensitivity of the orientation of the end-effector along Q_1Q_2, (a): to dimensional variations, (b): to angular variations

Figures 22(a-b) depict the sensitivity of the orientation of the end effector, along Q_1Q_2, to dimensional and angular variations. According to Fig.22(a), δl_i and δm_i are the only dimensional variations, which are responsible for the orientation error of the end-effector. However, the influence of the parallelism error of the small sides of the parallelograms, depicted by δl_i, is more important than the one of the parallelism error of their long sides, depicted by δm_i.

According to figures 21 and 22, the sensitivity of the position and the orientation of the end-effector is generally null in the kinematic isotropic configuration ($p = 0$), and is a maximum when the manipulator is close to a kinematic singular configuration, *i.e.*: $P \equiv Q_2$. Indeed, only two kinds of design parameters variations are responsible for the variations in the position of the end-effector in the isotropic configuration: δL_i and δe_{ix}. Likewise, two kinds of variations are responsible for the variations in its orientation in this configuration: δl_i, the parallelism error of the small sides of the parallelograms, $\delta\theta_{Aiy}$ and $\delta\gamma_{iy}$. Moreover, the sensitivities of the pose (position and orientation) of the end-effector to these variations are a minimum in this configuration, except for δl_i. On the contrary, Q_2 configuration, *i.e.*: $P \equiv Q_2$, is the most sensitive configuration of the manipulator to variations in its design parameters. Indeed, as depicted by Figs.21 and 22, variations in the pose of the end-effector depend on all the design parameters variations and are a maximum in this configuration.

Moreover, figures 21 and 22 can be used to compute the variations in the position and the orientation of the end-effector with knowledge of the amount of variations in design parameters. For instance, let us assume that the parallelism error of the small sides of the parallelograms, δl_i, is equal to 10μm. According to Fig.22(a), the position error of the end-effector will be equal about to 3μm in Q_1 configuration ($P \equiv Q_1$). Likewise, according to Fig.21(b), if the orientation error of the direction of the i^{th} prismatic joint round axis y_i of $\mathcal{R}_i$ is equal to 1 degree, *i.e.*: $\delta\theta_{Aiy} = 1$ degree, the position error of the end-effector will be equal about to 4.8 mm in Q_2 configuration.

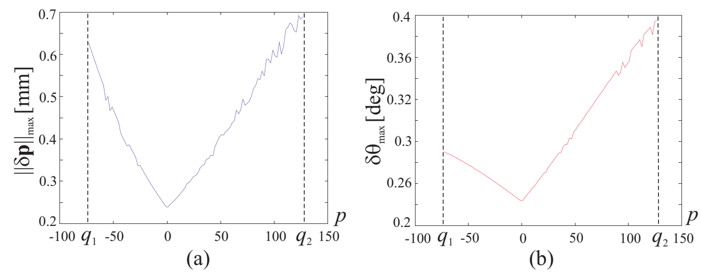

Figure 23. Maximum position (a) and orientation (b) errors of the end-effector along Q_1Q_2

Let us assume now that the length and angular tolerances are equal to 0.05 mm and 0.03 deg, respectively. Figure 23(a) shows the maximum position error of the end effector when it follows diagonal Q_1Q_2 of cube C_u. Likewise, Fig.23(b) shows the maximum orientation error of the end effector along Q_1Q_2. On both sides, the error is a minimum when the manipulator is in its kinematic isotropic configuration and is a maximum in Q_2 configuration. Besides, the maximum position and orientation errors of the end-effector are equal to 0.7 mm and 0.4 deg, respectively. These values correspond to the worst case scenario, which is unlikely.

Then, in order to take into account realistic machining tolerances, let us assume that the distribution of length and angular variations is normal.

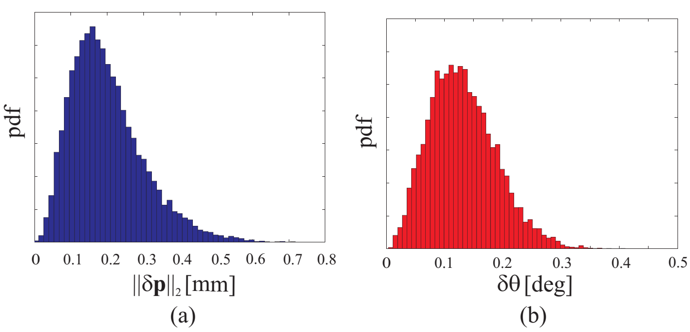

Figure 24. Repartition of the position error (a) and the orientation error (b) of the end-effector in Q_1 configuration

Figures 24 (a) and (b) illustrate the repartition of the position and the orientation errors of the end-effector in Q_1 configuration, respectively.

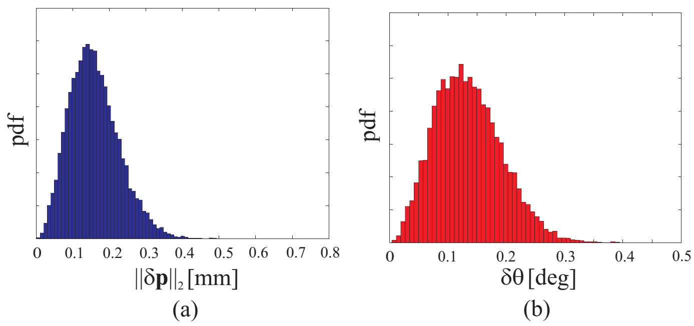

Figure 25. Repartition of the position error (a) and the orientation error (b) of the end-effector in the isotropic configuration

Figures 25 (a) and (b) illustrate the repartition of the position and the orientation errors of the end-effector in the kinematic isotropic configuration, respectively.

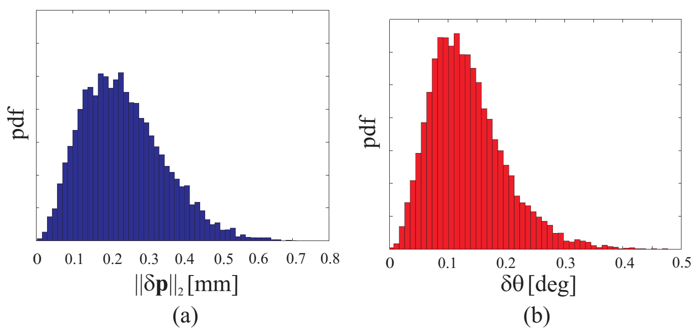

Figure 26. Repartition of the position error (a) and the orientation error (b) of the end-effector in Q_2 configuration

Figures 26 (a) and (b) illustrate the repartition of the position and the orientation errors of the end-effector in Q_2 configuration, respectively.

In Figures 24, 25, 26 (a) ((b), resp.) , the horizontal axis depicts the Euclidean norm of the position (orientation, resp.) error of the end-effector and the vertical axis depicts the corresponding probability density function (pdf). To plot these figures, we computed the position and orientation errors of the end-effector corresponding to more than three thousands sets of geometric variations following a normal distribution. For example, we can deduce from these calculations the probabilities to get a position error lower than 0.3 mm and an orientation error lower than

0.25 deg in Q_1, the isotropic, and Q_2 configurations.

	Configuration		
	Q_1	Isotropic	Q_2
$\mathrm{Prob}(\|\|\delta_p\|\|_2 \leq 0.3 \text{ mm})$	0.8468	0.9683	0.7276
$\mathrm{Prob}(\delta\theta \leq 0.25 \text{ deg})$	0.9691	0.9690	0.9453

Table 1. Probabilities to get a position error lower than 0.3 mm and an orientation error lower than 0.25 deg in Q_1, the isotropic, and Q_2 configurations

According to Table 1, the probability to get a position error lower than 0.3 mm is higher in the kinematic isotropic configuration than in Q_1 and Q_2 configurations. However, the probability to get an orientation error lower than 0.25 deg is the same in Q_1 and the isotropic configurations, but is lower in Q_2 configuration.

4 Conclusions

In this paper, two complementary methods were introduced to analyze the sensitivity of a three degree-of-freedom (DOF) translational Parallel Kinematic Machine (PKM) with orthogonal linear joints: the Orthoglide. Although these methods were applied to a particular PKM, they can be readily applied to 3-DOF Delta-Linear PKM such as ones with their linear joints parallel instead of orthogonal. Indeed, the input-output equations can be set in a very similar way since all Delta-linear PKM have identical leg kinematics, the only difference being in the closure equations [14].

On the one hand, a linkage kinematic analysis method was proposed to have a rough idea of the influence of the length variations of the manipulator on the location of its end-effector. On the other hand, a differential vector method was developed to study the influence of the length and angular variations in the parts of the manipulator on the position and orientation of its end-effector. This method has the advantage of taking into account the variations in the parallelograms.

According to the first method, variations in design parameters of the same type from one leg to another have the same effect on the end-effector. Besides, the position of the end-effector is very sensitive to variations in the lengths of parallelograms and prismatic joints. The second method shows that the parallelism errors of the bars of parallelograms are little influential on the position of the end-effector. Nevertheless, the orientation of the end-effector of the manipulator is more sensitive to the parallelism errors of the small sides of the parallelograms than to the ones of their long sides. Furthermore, it turns out that the sensitivity of the pose of the end-effector of the manipulator to geometric variations is a minimum in its kinematic isotropic configuration. On the contrary, this sensitivity approaches its maximum close to the kinematic singular configurations of the manipulator.

Therefore, these results should help the designer of the Orthoglide to synthesize its dimensional tolerances. Likewise, these methods can be applied to other Delta-Linear PKM with an aim of tolerance synthesis. Finally, the next steps in our research work are to compare the sensitivity of Delta-Linear PKM to variations in their geometric parameters, and to study the relation between the sensitivity and the stiffness of such manipulators.

ACKNOWLEDGMENT

This research, which is part of *ROBEA-MP2* project, was supported by the CNRS (National Center of Scientific Research in France).

REFERENCES

[1] Wenger, P., Gosselin, C., and Maillé, B., 1999, *A Comparative Study of Serial and Parallel Mechanism Topologies for Machine Tool*, Int. Workshop on Parallel Kinematic Machines, Milan, Italie, pp. 23-35.

[2] Wang, J., and Masory, O., 1993, *On the accuracy of a Stewart platform - Part I, The effect of manufacturing tolerances.*, In: Proceedings of the IEEE International Conference on Robotics Automation, ICRA'93, Atlanta, USA, pp. 114-120.

[3] Kim, H.S., and Choi, Y.J., 2000, *The kinematic error bound analysis of the Stewart platform*, Journal of Robotic Systems, **17**, pp. 63-73.

[4] Kim, H.S., and Tsai, L-W., 2003, *Design optimization of a Cartesian parallel manipulator*, ASME J. Mech. Des., **125**, pp. 43-51.

[5] Han, C., Kim, Ji., Kim, Jo., and Park F.C., 2002, *Kinematic sensitivity analysis of the 3-UPU parallel mechanism*, Mechanism and Machine Theory, **37**, pp. 787-798.

[6] Fan, K-C., Wang, H., Zhao, J-W., and Chang T-H., 2003, *Sensitivity analysis of the 3-PRS parallel kinematic spindle platform of a serial-parallel machine tool*, International Journal of Machine Tools & Manufacture, **43**, pp. 1561-1569.

[7] Verner, M., Fengfeng, X., and Mechefske, C., 2005, *Optimal Calibration of Parallel Kinematic Machines*, ASME J. Mech. Des., **127**, pp. 62-69.

[8] Caro, S., Bennis, F., and Wenger, P., 2005, *Tolerance Synthesis of Mechanisms: A Robust Design Approach*, ASME J. Mech. Des., **127**, pp. 86-94.

[9] Chablat, D., and Wenger, P., 2003, *Architecture Optimization of a 3-DOF Parallel Mechanism for Machining Applications, The Orthoglide*, IEEE Transactions On Robotics and Automation, **19**, pp. 403-410.

[10] Zanganeh, K.E., and Angeles, J., 1994, *Kinematric isotropy and the optimum design of parallel manipulators*, Int. J. of Rob. Research, **16**, No.2, pp. 3-9.

[11] Karouia, M., and Herve, J.M., 2002, *A family of novel orientational 3-dof parallel robots*, Proceedings of the 14^{th} CISM-IFToMM RoManSy Symposium, RoMansSy 14. (Edited by G. Bianchi, J.C. Guinot and Rzymkowski), Springer Verlag. Vienna, pp. 359-368.

[12] Huang, T., Whitehouse, D.J., and Chetwynd, D.G., 2003, *A Unified Error Model for Tolerance Design, Assembly and Error Compensation of 3-DOF Parallel Kinematic Machines with Parallelogram Sruts*, Science in China Series E, ISSN:1006-9321, 20, **46**, No.5, pp. 515-526.

[13] Angeles, J., 2002, *Fundamentals of Robotic Mechanical Systems*, Springer-Verlag, New-York, 2^{nd} edition.

[14] Chablat, D., Wenger, P., Majou, F., and Merlet, J.P., 2004, *An Interval Analysis Based Study for the Design and the Comparison of 3-DOF Parallel Kinematic Machines*, International Journal of Robotics Research, **23**, No.6, June, pp. 615-624.